Prospects for supersymmetry at CERN LEP 2

Howard Baer,[1] Michal Brhlik,[1] Ray Munroe,[1] and Xerxes Tata[2]
[1]*Department of Physics, Florida State University, Tallahassee, Florida 32306*
[2]*Department of Physics and Astronomy, University of Hawaii, Honolulu, Hawaii 96822*
(Received 29 June 1995)

Working within the framework of the minimal supergravity (SUGRA) model with gauge coupling unification and radiative electroweak symmetry breaking we map out regions of parameter space explorable by experiments at CERN LEP 2, for center-of-mass energy options of $\sqrt{s} = 150$, 175, 190, and 205 GeV. We compute signals from all accessible $2 \to 2$ supersymmetry (SUSY) pair production processes using the ISAJET simulation program, and devise cuts that enhance the signal relative to standard model backgrounds, and which also serve to differentiate various supersymmetric processes from one another. We delineate regions of SUGRA parameter space where production of neutralino pairs, chargino pairs, slepton pairs, and the production of the light Higgs scalar of SUSY is detectable above standard model backgrounds and distinguishable from other SUSY processes. In addition, we find small regions of SUGRA parameter space where $\tilde{e}\tilde{e}$, $\widetilde{Z}_2\widetilde{Z}_2$, and $\tilde{\nu}_L\tilde{\nu}_L$ production yields spectacular events with up to four isolated leptons. The combined regions of parameter space explorable by LEP 2 are compared with the reach of Fermilab Tevatron Main Injector era experiments. Finally, we comment on how the reach via the neutralino pair channel is altered when the radiative electroweak symmetry breaking constraint is relaxed.

PACS number(s): 14.80.Ly, 11.30.Pb, 13.85.Qk

I. INTRODUCTION

The CERN e^+e^- collider LEP, currently running with total center-of-mass energy around the Z pole, is expected to undergo an energy upgrade in the near future, to become LEP2. The machine energy will ultimately exceed the WW production threshold so that experiments at LEP2 will directly probe the form of the ZWW and the γWW interactions [1]. The higher energy and the clean experimental environment of LEP2 will also allow direct searches for new particles, including the Higgs boson, the expected relic of the spontaneous breaking of the electroweak gauge group. Another important goal of LEP2 experiments is the direct search for new particles that occur in various extensions of the standard model (SM), the most promising of which is low energy supersymmetry [2,3]. Already, the four LEP experiments have placed relatively model independent bounds on the masses of various sparticles and Higgs bosons [4]. To be specific [5],

$$
\begin{aligned}
&m_{\widetilde{W}_1} > 45 \text{ GeV},\\
&m_{\tilde{\ell}} > 45 \text{ GeV} \quad (\tilde{\ell} = \tilde{e}, \tilde{\mu}, \tilde{\tau})\\
&m_{\tilde{q}} > 45 \text{ GeV},\\
&m_{\tilde{\nu}} > 41.8 \text{ GeV} \quad \text{(three degenerate flavors)}\\
&m_{H_\ell} > 44 \text{ GeV} \quad (\text{for } \tan\beta > 1),
\end{aligned}
$$

where $\widetilde{W}_1$ is the lightest chargino and H_ℓ is the lightest neutral scalar in the Higgs sector. The above sparticle mass limits are mainly limited by the beam energy. Hence, considerable improvement is expected at LEP 2. In addition, the Collider Detector at Fermilab (CDF) and D0 Collaborations, from a nonobservation of any excess of $\not{E}_T$ events at the Fermilab Tevatron $p\bar{p}$ collider, now require [6]

$$
\begin{aligned}
&m_{\tilde{g}} > 150 \text{ GeV},\\
&m_{\tilde{q}} > 150 \text{ GeV} \quad (\text{if } m_{\tilde{g}} \lesssim 400 \text{ GeV}).
\end{aligned}
$$

The Tevatron bounds have been obtained within the framework of the minimal supersymmetric model (MSSM) and are somewhat sensitive to the assumed unification of gaugino masses, but depend only weakly on other SUSY parameters.

Many previous LEP analyses [7,8] (including the experimental ones) have been performed within the framework of the supergravity-inspired MSSM. The weak scale sparticle masses are assumed to originate from unification scale common soft-breaking terms m_0 (for scalar sparticles) and $m_{1/2}$ (for gaugino masses). Thus the first five flavors of squarks are assumed to be approximately degenerate, as are the sleptons. The soft-breaking trilinear coupling A_t mainly affects the mass and the phenomenology of top squarks, and is neglected for most purposes. The ratio $\tan\beta$ of the two Higgs boson field vacuum expectation values, the SUSY-conserving superpotential Higgs boson mass μ, and finally, the pseudoscalar Higgs boson mass m_{H_p} are taken to be free parameters. These analyses generally focus upon the production of just one sparticle species at a time, although 31 new particles are predicted, and it is possible to have several closely spaced thresholds.

Recently, several groups [9–14] have studied SUSY phenomenology at colliders within the framework of the highly constrained minimal supergravity (SUGRA) grand unified model, with gauge coupling unification

and radiative electroweak symmetry breaking. SUGRA models should be regarded as effective theories with Lagrangian parameters renormalized at an ultrahigh scale $M_X \sim M_{\rm GUT} - M_{\rm Planck}$, and valid only below this scale. The corresponding weak scale sparticle coupling and masses are then calculated by evolving 26 renormalization group equations [15] from the unification scale to the weak scale. An elegant by-product [16] of this mechanism is that one of the Higgs boson mass squared terms is driven negative, resulting in a breakdown of electroweak symmetry. This model is completely specified by four [17] SUSY parameters (in addition to SM masses and couplings). A hybrid set consisting of the common mass m_0 ($m_{1/2}$) for all scalars (gauginos), a common SUSY-breaking trilinear coupling A_0 all specified at the scale M_X together with $\tan\beta$ proves to be a convenient choice. These parameters fix the masses and couplings of all sparticles. In particular, m_{H_p} and the magnitude (but not the sign) of μ are fixed. In other words, various assumptions about the symmetries of interactions at the scale M_X that have been built into the SUGRA framework restrict the model parameters to a subset of the SUGRA-inspired MSSM parameter space referred to earlier. We note that sparticle signatures for LEP2 have been discussed (without explicit event generation) within the more restrictive framework of constrained SU(5) and flipped SU(5) models in Ref. [9].

The SUGRA framework (and also a SUGRA-inspired MSSM framework without radiative elecroweak symmetry breaking) has been incorporated into the event generator program ISAJET 7.13 [12,18]. All lowest order $2 \to 2$ sparticle and Higgs boson production mechanisms have been incorporated into ISAJET. These include the processes (neglecting bars over antiparticles)

$$
\begin{aligned}
&e^+e^- \to \tilde{q}_L\tilde{q}_L,\ \tilde{q}_R\tilde{q}_R,\\
&e^+e^- \to \tilde{\ell}_L\tilde{\ell}_L,\ \tilde{\ell}_R\tilde{\ell}_R,\ \tilde{e}_L\tilde{e}_R,\\
&e^+e^- \to \tilde{\nu}_\ell\tilde{\nu}_\ell,\\
&e^+e^- \to \widetilde{W}_1\widetilde{W}_1,\ \widetilde{W}_2\widetilde{W}_2,\ \widetilde{W}_1\widetilde{W}_2,\\
&e^+e^- \to \widetilde{Z}_i\widetilde{Z}_j\ \ (i,j=1-4),\\
&e^+e^- \to ZH_\ell,\ ZH_h,\ H_pH_\ell,\ H_pH_h,\ H^+H^-.
\end{aligned}
$$

In the above, $\ell = e$, μ, or τ. All squarks (and also all sleptons other than staus) are taken to be L or R eigenstates, except the stops, for which $\tilde{t}_1\tilde{t}_1$, $\tilde{t}_1\tilde{t}_2$, and $\tilde{t}_2\tilde{t}_2$ (here, $\tilde{t}_{1,2}$ being the lighter and/or heavier of the top squark mass eigenstates) production is included. Given a point in SUGRA space, and a collider energy, ISAJET generates all allowed production processes, according to their relative cross sections. The produced sparticles or Higgs bosons are then decayed into all kinematically accessible channels, with branching fractions calculated within ISAJET. The sparticle decay cascade terminates with the lightest SUSY particle (LSP), taken to be the lightest neutralino ($\widetilde{Z}_1$). Final state QCD radiation is included, as well as particle hadronization. ISAJET currently neglects spin correlations, sparticle decay matrix elements, and also, initial state photon radiation. In the above reactions, spin correlation effects are only important for chargino and neutralino pair production, while decay matrix elements are only important for three-body sparticle decays.

The purpose of this paper is threefold.

(1) We examine SUSY signals in the highly restricted SUGRA framework. We note that frequently one must consider not just a single SUSY production mechanism, but rather one must often consider simultaneously production of several different sparticles, since their masses are expected to be correlated. For the purposes of sparticle detection, this means that not only should signals be observable above SM backgrounds, but also that two or more signals have to be untangled from one another if they happen to occur simultaneously.

(2) We examine how the regions of SUGRA parameter space for sparticle or Higgs boson detection alter as a function of the machine energy and luminosity. We are motivated by the possibility that it may be feasible to increase the energy of LEP2 from its starting value of about 140–150 GeV. The options considered are

$$
\begin{aligned}
&\sqrt{s} = 150\ \text{GeV}, \quad \int \mathcal{L}dt = 500\ \text{pb}^{-1},\\
&\sqrt{s} = 175\ \text{GeV}, \quad \int \mathcal{L}dt = 500\ \text{pb}^{-1},\\
&\sqrt{s} = 190\ \text{GeV}, \quad \int \mathcal{L}dt = 300\ \text{pb}^{-1},\\
&\sqrt{s} = 205\ \text{GeV}, \quad \int \mathcal{L}dt = 300\ \text{pb}^{-1}.
\end{aligned}
$$

The first of these cases is of special interest [7,8] because, below the WW threshold, SM backgrounds are frequently tiny.

(3) There are regions of parameter space where the only visible sparticle production could come from $\widetilde{Z}_1\widetilde{Z}_2$ production. Within the MSSM, the rate for this reaction can be very small if the neutralinos are mainly gaugino-like and sleptons heavy, which is probably why this reaction has not been studied in as much detail as chargino or slepton pair production in the earlier literature. We examine the prospects of identifying signals from this reaction over SM backgrounds and further, of discriminating $\widetilde{Z}_1\widetilde{Z}_2$ production from other SUSY and Higgs production processes.

As an illustration of (1) above, we show in Fig. 1 total sparticle production cross sections at $\sqrt{s} = 175$ GeV versus the unification scale gaugino mass $m_{1/2}$. We take $A_0 = 0$, $\tan\beta = 2$ and $\mu < 0$. In Fig. 1(a), we take $\xi = \frac{m_0}{m_{1/2}} = 0$, and begin the lower limit of our plot from $m_{1/2} \sim 90$ GeV, below which the sneutrino mass violates the above LEP bounds [Eq. (1)]. For $m_{1/2} < 140$ GeV, pair production of L and R selectrons is dominant, although $\sigma(e^+e^- \to ZH_\ell) \sim 1000$ fb. In addition, smuon and stau pair production is taking place at $\sigma \sim 500$ fb. Chargino pair production is kinematically forbidden but $\sigma(e^+e^- \to \widetilde{Z}_2\widetilde{Z}_1) \sim 200$–$400$ fb, when $m_{1/2}$ is small. In this case, the neutralino pair signals may be difficult to extract from a background which includes *other* SUSY and Higgs boson processes. In Fig. 1(b), we take $\xi = 1$. In this case, sleptons are too heavy to be produced and the dominant new-particle cross section comes from

ZH_ℓ production, followed by $\widetilde{Z}_2\widetilde{Z}_1$ and $\widetilde{W}_1\overline{\widetilde{W}_1}$ production (which just becomes accessible) when $m_{1/2}$ is small. Finally, in Fig. 1(c) we take $\xi = 4$. Now, because smaller values of $m_{1/2}$ are not excluded by LEP experiments, $\widetilde{W}_1\overline{\widetilde{W}_1}$ production is dominant out to $m_{1/2} = 90$ GeV, followed by ZH_ℓ production. The production of $\widetilde{Z}_2\widetilde{Z}_1$ events occurs at a very low rate, and would be difficult to separate from the $\widetilde{W}_1\overline{\widetilde{W}_1}$ pair signals, as well as the SM WW background.

The remainder of this paper is organized as follows. In Secs. II, III, and IV, we describe our analyses for the extraction of various signals at center of mass energies of 150, 175, and 190–205 GeV, respectively. Because WW and ZZ (ZZ) production is kinematically inaccessible in the first (second) case, SM physics backgrounds (and hence the cuts we choose to extract the signal) differ in the three cases. The reader who is not interested in the details of the analysis need focus only on the results presented in the figures and the accompanying discussion, but can skip over the details of the selection criteria detailed therein. In Sec. V, we discuss additional signals such as 4ℓ production via, e.g., $\tilde{\nu}_\ell\overline{\tilde{\nu}_\ell}$, $\tilde{e}\overline{\tilde{e}}$, or $\widetilde{Z}_2\widetilde{Z}_2$ production, which do not necessarily extend the parameter space reach, but do yield exotic, gold-plated signatures for sparticle production reactions that are usually neglected in the literature. In Sec. VI we compare the reach of the various LEP2 upgrade options amongst themeselves, and with the capabilities of the Fermilab Tevatron Main Injector upgrade. In Sec. VII, we discuss how neutralino signals (in particular) are altered if the constraint from radiative electroweak symmetry breaking is relaxed. The latter allows $|\mu|$ to become a free parameter, so that the lighter $\widetilde{Z}_i$ can have large higgsino components. We focus mainly on neutralino production because pair production of charged sparticles is less model dependent, and their signals have also been extensively [7,8] studied within the SUGRA-inspired MSSM framework. We conclude with a summary of our results in Sec. VIII.

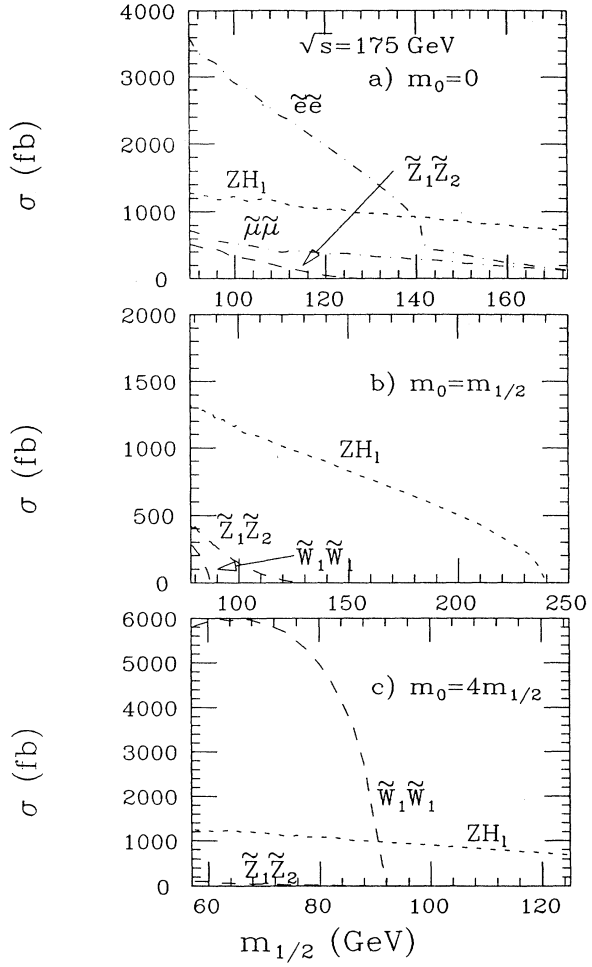

FIG. 1. Total cross sections vs common GUT scale gaugino mass $m_{1/2}$ for various particle creation mechanisms within the minimal SUGRA model, for e^+e^- reactions at $\sqrt{s} = 175$ GeV. We take $A_0 = 0$, $\tan\beta = 2$ and $\mu < 0$. In (a), we show results for $m_0 = 0$, while in (b) we show results for $m_0 = m_{1/2}$, and in (c) we take $m_0 = 4m_{1/2}$.

II. SPARTICLE SIGNALS AT $E_{\rm c.m.} = 150$ GeV

The first test run of LEP2 is expected to begin in late 1995, with collider energy of $\sqrt{s} \sim 140 - 150$ GeV. A major feature of a collider run at this energy is that it is still below threshold for WW production, and SM backgrounds to signals from the production of new, heavy particles are small. Indeed, if hints of new physics signal are seen, then collection of substantial integrated luminosity below WW threshold may be desirable [7,8]. Furthermore, in this energy range, one does not expect to produce the light Higgs scalar H_ℓ. In the minimal SUGRA model, where $|\mu|$ (derived from radiative electroweak symmetry breaking) is typically large, $H^\pm$, H_h, and H_p are very heavy, whereas the light Higgs scalar is expected to be nearly indistinguishable from a SM Higgs scalar. Hence, except in some corners of parameter space, LEP limits of $m_{H_{\rm SM}} \gtrsim 60$ GeV apply as well to H_ℓ, so that a collider energy of $\sqrt{s} > m_Z + 60$–150 GeV will be needed to probe new territory in the Higgs sector. The reactions to focus on at $\sqrt{s} \sim 150$ GeV are then (i) $\tilde{\ell}_i\overline{\tilde{\ell}_i}$ production (where $\tilde{\ell} = e$, μ, or τ, and $i = L$ or R), (ii) $\widetilde{W}_1\overline{\widetilde{W}_1}$ production, and (iii) $\widetilde{Z}_1\widetilde{Z}_2$ production.

We do not consider squark signals in this paper, since squarks light enough to be accessible at LEP2 are already excluded by hadron collider data. A possible exception is the light $\tilde{t}_1$ for which the hadron collider limits are not applicable. The best limit on $m_{\tilde{t}_1}$ come from LEP experiments, so that LEP2 should be able to probe beyond the current bounds. With a data sample of about 100 pb^{-1} the Tevatron experiments will also be able to probe [19] $\tilde{t}_1$ masses up to 80–100 GeV. For this reason, and because $m_{\tilde{t}_1}$ is rarely lighter than 100 GeV in SUGRA parameter space, we do not consider top squark signals any further in this paper.

2.1 selectrons. Although potentially any of the slepton pair reactions (e.g., $\tilde{e}_R\overline{\tilde{e}_R}$, $\tilde{e}_R\overline{\tilde{e}_L}$, $\tilde{e}_L\overline{\tilde{e}_R}$, $\tilde{e}_L\overline{\tilde{e}_L}$, $\tilde{\mu}_R\overline{\tilde{\mu}_R}$, $\tilde{\mu}_L\overline{\tilde{\mu}_L}$, $\tilde{\tau}_1\overline{\tilde{\tau}_1}$, $\tilde{\tau}_2\overline{\tilde{\tau}_2}$) can occur at LEP, we focus only on

the selectron pair production reactions. Unlike smuon or stau production which occurs only via s-channel γ and Z exchanges, selectron pair production can also occur via the exchange of neutralinos in the t channel. Because the left- (right-) slepton masses are expected to be independent of flavor (except for negligible effects from the differences in Yukawa interactions), the additional t-exchange contributions generally result in larger cross sections for selectron pair production than for the production of smuon or stau pairs [7,8]. As a result, smuons and staus can usually be detected in a subset of the parameter space where selectrons are observable, although for very large values of $\tan\beta$ where the stau mixing induced by tau Yukawa interactions becomes important, it is possible that $\tilde{\tau}_1\bar{\tilde{\tau}}_1$ production is the only accessible slepton production process.

Selectron pair production usually results in a very clean event containing an acollinear e^+e^- pair plus missing energy. Below the WW threshold, the main backgrounds come from (i) $\tau^+\tau^-$ production followed by the leptonic decays of the τ's, (ii) $e^+e^-\gamma$ production, where the photon is lost down the beam pipe, and (iii) $e^+e^-e^+e^-$ production via two photon reactions. It has been shown that [8] requiring $\not{E}_T > \sqrt{s}\sin\theta_{\min}/(1+\sin\theta_{\min})$, where $\theta_{\min}$ is the minimum angle above which leptons and photons can be efficiently detected, very effectively eliminates background from processes (ii) and (iii). At LEP2 energies, the leptons from $\tau^+\tau^-$ production are essentially back-to-back in the transverse plane. To quantify the size of the signal and the τ pair background, we generate selectron pair events as well as $\tau^+\tau^-$ background using ISAJET. We require

$$E_\ell > 3 \text{ GeV}, \quad |\eta_\ell| < 2.5, \tag{2.1}$$

$$\not{E}_T > 7.5 \text{ GeV}, \tag{2.2}$$

$$\cos\phi(\ell^+\ell^-) > -0.9. \tag{2.3}$$

After these cuts, we are left with no significant SM background at $\sqrt{s} = 150$ GeV. We then (conservatively) require 10 signal events to claim discovery.

The regions of selectron observability in SUGRA parameter space are plotted in the m_0 vs $m_{1/2}$ plane in Fig. 2, where we take $A_0 = 0$ and $m_t = 170$ GeV. In Fig. 2(a), we show results for $\tan\beta = 2$ and $\mu < 0$, while in Fig. 2(b) we take the same $\tan\beta = 2$ but require $\mu > 0$. Finally, in Fig. 2(c), we take $\tan\beta = 10$ with $\mu < 0$, and in Fig. 2(d) we take $\tan\beta = 10$ with $\mu > 0$. Regions excluded by theoretical constraints such as lack of appropriate electroweak symmetry breaking, or where the LSP is not $\widetilde{Z}_1$, are enclosed by solid contours, and labeled TH. Similarly, regions excluded by various LEP constraints ($m_{\widetilde{W}_1} < 47$ GeV [20], $m_{\tilde{\nu}} < 43$ GeV, $m_{H_\ell} < 60$ GeV) and Tevatron constraints from multijets+$\not{E}_T$ searches are denoted by EX. The regions of selectron observability are denoted by dashed contours in the low m_0 region. Generally, selectrons are observable over most of the region where their production is kinematically allowed. An exception to this, however, occurs around $m_0 \sim 0$, and $m_{1/2} \sim 150$ GeV in case (a) where the contour turns over. In this region, the mass difference $m_{\tilde{\ell}_R} - m_{\widetilde{Z}_1}$ becomes so small that there is not enough visible energy from the selectron decays to yield an observable signal.

2.2 charginos. The chargino pair production cross section is typically in a few pb range when chargino pair production is kinematically allowed, although it may be significantly suppressed when $m_{\tilde{\nu}} \sim \frac{\sqrt{s}}{2}$. Chargino pair signals occur in the multijet $+\not{E}_T$ channel, the mixed ℓ+jet(s)+$\not{E}_T$ channel, and the $\ell\bar{\ell}' + \not{E}_T$ channel, any of which might be readily observable when LEP2 is operating below WW threshold. The cuts below have been suggested [21] for a chargino search when $\widetilde{W}_1\bar{\widetilde{W}}_1 \to \ell\nu\widetilde{Z}_1 + q\bar{q}'\widetilde{Z}_1$. Although these cuts are optimized for a chargino search above WW threshold, they generally allow a search for charginos up to threshold even for $\sqrt{s} \sim 150$ GeV. Hence, we require,

No. charged particles > 5, (2.4)

$\not{E}_T > 10$ GeV, (2.5)

Isolated e or μ with $E_\ell > 5$ GeV, (2.6)

Missing mass > 63 GeV, (2.7)

Mass of the hadronic system < 45 GeV, (2.8)

$m(\ell\nu) < 70$ GeV. (2.9)

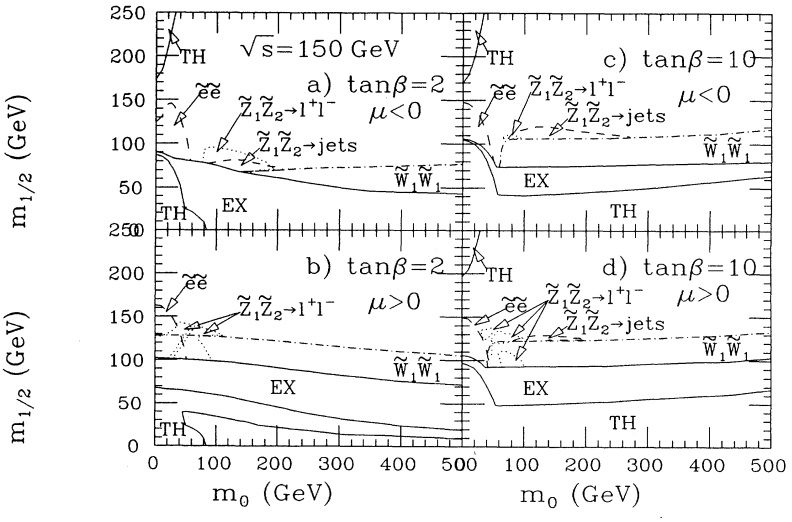

FIG. 2. Regions of the m_0 vs $m_{1/2}$ plane explorable at LEP2 with $\sqrt{s} = 150$ GeV, and $\int \mathcal{L}dt = 500$ pb^{-1}. In all frames, we take $A_0 = 0$. In (a), we take $\tan\beta = 2$, $\mu < 0$, while in (b) we take $\tan\beta = 2$ with $\mu > 0$. In (c), we take $\tan\beta = 10$, $\mu < 0$ and in (d) we take $\tan\beta = 10$, $\mu > 0$. The regions denoted by TH are excluded by theoretical constraints, while the region labeled EX is excluded by experimental constraints.

The ten event regions where the signal is nominally taken to be observable are below the dot-dashed contours in Fig. 2, and roughly follow the contour of constant $m_{1/2}$. The notable exceptions occur in Figs. 2(c) and 2(d), where the dot-dashed contour turns down at $m_0 \sim 50$ GeV. Below this value of m_0, the decay mode $\widetilde{W}_1 \to \tilde{\nu}_{\ell L}\ell$ turns on, so only the $\widetilde{W}_1\overline{\widetilde{W}_1} \to \ell\bar{\ell}' + \not{E}_T$ mode occurs. If $m_{\tilde{\nu}_{\ell L}} \sim m_{\widetilde{W}_1}$, then the final state leptons are very soft, and may be difficult to detect. For even lower values of m_0, the sneutrinos become even lighter, and the purely leptonic channel from chargino pair production can fill in *part* of the gap between the selectron contour and the dashed-dotted chargino pair contour.

2.3 neutralinos. Neutralino pair production occurs via s-channel Z exchange and t- and u-channel L- and R-selectron exchange graphs. In minimal SUGRA models, where $m_{\widetilde{Z}_1} \sim \frac{1}{2}m_{\widetilde{Z}_2}$ and $m_{\widetilde{Z}_2} \sim m_{\widetilde{W}_1}$, there exists a region of parameter space where $\widetilde{Z}_1\widetilde{Z}_2$ is kinematically accessible but $\widetilde{W}_1\overline{\widetilde{W}_1}$ production is forbidden. Moreover, the two lightest neutralinos are mainly gaugino-like, with small coupling to the Z boson, resulting in a suppressed contribution from the s-channel graph. In addition, t-channel $\widetilde{Z}_1\widetilde{Z}_2$ production is suppressed when $m_{\tilde{e}_i}$ is heavy, but can be significant if $m_{\tilde{e}_i}$ is light (m_0 small). Once produced, the $\widetilde{Z}_2$ can decay via real or virtual Z, H_i, $\tilde{\ell}_i$, $\tilde{\nu}$, or $\tilde{q}_i$. The most promising signatures include $\widetilde{Z}_1\widetilde{Z}_2 \to \ell\bar{\ell} + \not{E}_T$ and $\widetilde{Z}_1\widetilde{Z}_2 \to q\bar{q} + \not{E}_T$. We have evaluated $e^+e^- \to \widetilde{Z}_1\widetilde{Z}_2$ along with decays without spin correlations (using ISAJET), and with spin correlations (using HELAS [22]), and find little difference between the final signal rates. We attribute this to the fact that for SUGRA parameter space regions where the signal is observable $\widetilde{Z}_1\widetilde{Z}_2$ production is dominated by slepton exchange, while decays are dominated by squark, slepton, and sneutrino exchange—all spin-0 particles.

To search for $e^+e^- \to \widetilde{Z}_1\widetilde{Z}_2 \to \ell\bar{\ell} + \not{E}_T$ events, we require

$$E_\ell > 3 \text{ GeV}, \quad |\eta_\ell| < 2.5, \tag{2.10}$$
$$\not{E}_T > 7.5 \text{ GeV}, \tag{2.11}$$
$$\not{E} > 89 \text{ GeV}, \tag{2.12}$$
$$m(\ell\bar{\ell}) < 55 \text{ GeV}, \tag{2.13}$$
$$\phi(\ell_1, \ell_2) < 172^\circ. \tag{2.14}$$

These allow one to see the dilepton signal above the SM $\tau\bar{\tau}$ background, and also above the dilepton level expected from $\widetilde{W}_1\overline{\widetilde{W}_1}$ production. The resulting ten-event signal level is plotted in Figs. 2(a)–2(d) as the dotted contour. In Fig. 2(a), we see that $\widetilde{Z}_1\widetilde{Z}_2 \to \ell\bar{\ell} + \not{E}_T$ is visible mainly for $80 \lesssim m_0 \lesssim 210$ GeV, for values of $m_{1/2}$ ranging up to ~ 100 GeV—well beyond the reach for chargino pairs. For smaller values of m_0, the signal is not observable because $\widetilde{Z}_2$ dominantly decays invisibly to $\nu\bar{\nu}$. In Fig. 2(b), the $\widetilde{Z}_1\widetilde{Z}_2 \to \ell\bar{\ell} + \not{E}_T$ signal should be detectable for small values of m_0 as well because here, $\widetilde{Z}_2 \to \ell\tilde{\ell}_R$ decays dominate. Note the small diagonal gap between the two disjoint dilepton regions: here the $\widetilde{Z}_2 \to \ell\tilde{\ell}_R$ decays dominate, but are just barely open, and result in one of the signal leptons being too soft to be observable. In Fig. 2(c), there is again a small region of observability for $\widetilde{Z}_1\widetilde{Z}_2 \to \ell\bar{\ell} + \not{E}_T$, but here it is limited to $60 < m_0 < 100$ GeV, and does not give much additional region of observability beyond the $\widetilde{W}_1\overline{\widetilde{W}_1}$ observability region. Finally, in Fig. 2(d), there exist three disjoint regions where $\widetilde{Z}_1\widetilde{Z}_2 \to \ell\bar{\ell} + \not{E}_T$ is visible.

To search for $\widetilde{Z}_1\widetilde{Z}_2 \to$ jets$+\not{E}_T$, we first coalesce hadronic clusters within a cone of $\Delta R < 0.5$, and label as a jet if $E_j > 5$ GeV and $|\eta_j| < 2.5$. In addition, we require

$$\not{E}_T > 7.5 \text{ GeV}, \tag{2.15}$$
$$m_{\text{jet}} > 5 \text{ GeV (monojet events)}, \tag{2.16}$$
$$\phi(j_1, j_2) < 172^\circ \text{ (dijet events)}. \tag{2.17}$$

We veto events with identified e or μ in them. The main SM background comes from $\tau\bar{\tau}$ production (recall that WW and ZH_ℓ production is inaccessible), and is essentially eliminated by the latter two cuts. However, in regions where $\widetilde{W}_1\overline{\widetilde{W}_1}$ is open, there is a large background from $\widetilde{W}_1\overline{\widetilde{W}_1} \to 1$ or 2 jets$+\not{E}_T$, due to double hadronic chargino decays where jets are soft or coalesce, and due to single hadronic chargino decays, where the other chargino decays to a hadronic τ or a soft or missing lepton. The latter supersymmetric background makes $\widetilde{Z}_1\widetilde{Z}_2 \to$ jets$+\not{E}_T$ very difficult to distinguish as an independent production and decay mechanism. In Figs. 2(a)–2(d), we show the region for hadronic $\widetilde{Z}_1\widetilde{Z}_2$ detection as short dashed contours. In Fig. 2(a), $\widetilde{Z}_1\widetilde{Z}_2 \to$ jets$+\not{E}_T$ is observable in a subset of the region where dileptons from $\widetilde{Z}_1\widetilde{Z}_2$ are visible. In Fig. 2(b), $\widetilde{Z}_1\widetilde{Z}_2 \to$ jets$+\not{E}_T$ is essentially not visible at all, while in Figs. 2(c) and 2(d), $\widetilde{Z}_1\widetilde{Z}_2 \to$ jets$+\not{E}_T$ is observable beyond the $\widetilde{W}_1\overline{\widetilde{W}_1}$ region in a small but not insignificant slice of parameter space.

III. SPARTICLE PRODUCTION AT $E_{\text{c.m.}} = 175$ GeV

LEP2, running at $\sqrt{s} = 175$ GeV, will be above threshold for WW production, for which the total cross section is $\sigma(WW) \sim 17.3$ pb. An extended run to gather $\int \mathcal{L}dt \sim 500$ pb^{-1} of integrated luminosity is expected to occur, to measure the W mass and triple vector boson coupling. Furthermore, at this energy, LEP2 will be sensitive to higher ranges of Higgs boson masses, up to $m_{H_{\text{SM}}} \sim 80$ GeV.

3.1 selectrons. Selectron pair production has an irreducible background now from $WW \to e^+\nu_e e^-\overline{\nu_e}$, which occurs at the 212 fb level. To reduce WW background, additional cuts are needed beyond those of (2.1)–(2.3):

$$3 < E_\ell < 46 \text{ GeV}, \quad |\eta_\ell| < 2.5, \tag{3.1}$$
$$\not{E}_T > 9 \text{ GeV}, \tag{3.2}$$
$$\cos\phi(\ell^+\ell^-) > -0.9, \tag{3.3}$$
$$\pm \cos\theta_{\ell^\pm} > 0, \tag{3.4}$$

where θ_ℓ is the angle between the beam and the detected lepton. The $\cos\theta$ cut is applied only to the more energetic of the two detected leptons.

To evaluate the background from WW production, we have used the HELAS package to calculate the spin-correlated Feynman diagrams for various final state configurations (thus, the WW and ZZ backgrounds are evaluated at the parton level). After the above cuts, we find backgrounds of

$$WW \to e^+e^- : \ 11.5 \text{ fb},$$
$$WW \to \tau^\pm e^\mp \to e^+e^- : \ 7.5 \text{ fb},$$
$$WW \to \tau^+\tau^- \to e^+e^- : \ 1.2 \text{ fb}.$$

We then plot in Fig. 3 dashed contours that mark the boundaries of the regions where the selectron signal exceeds background at the 5σ level. In Fig. 3(a), the reach can be as high as $m_{\tilde{\ell}_R} = 84$ GeV when $m_{\widetilde{Z}_1}$ is as light as 36 GeV, but is diminished when $m_{\widetilde{Z}_1}$ is heavier (large values of $m_{1/2}$).

3.2 charginos. Charginos are best searched for in the mixed hadronic-leptonic final state, e.g., $\widetilde{W}_1\widetilde{W}_1 \to \ell\nu_\ell\widetilde{Z}_1 + q\overline{q'}\widetilde{Z}_1$. Grivaz has suggested the set of cuts (2.4)–(2.9) as optimizing signal to background. Using these cuts, he estimates a background from WW and other SM processes of 9 fb. We map out the region yielding a 5σ signal above background as the dot-dashed contour in Figs. 3(a)–3(d). For large values of $m_0 \sim 500$ GeV, LEP2 at $\sqrt{s} = 175$ GeV can probe to $m_{\widetilde{W}_1} = 86.7$ GeV in Fig. 3(b). However, for low values of m_0, in Figs. 3(a), 3(c), and 3(d), the reach via chargino searches cuts off due to turn on of the two body decay $\widetilde{W}_1 \to \tilde{\nu}_{\ell L}\ell$, which then dominates the branching fraction.

3.3 neutralinos. The background from $WW \to \ell^+\ell^- + \not{E}_T$ forces a more severe set of cuts to search for $e^+e^- \to \widetilde{Z}_1\widetilde{Z}_2 \to \ell\bar{\ell} + \not{E}_T$ events. To reduce WW background, we require

$$10 < E_\ell < 40 \text{ GeV}, \quad |\eta_\ell| < 2.5, \tag{3.5}$$
$$\not{E}_T > 9 \text{ GeV}, \tag{3.6}$$
$$\not{E} > 105 \text{ GeV}, \tag{3.7}$$
$$m\,(\ell\bar{\ell}) < 50 \text{ GeV}, \tag{3.8}$$
$$m\!\!\!/ > 90 \text{ GeV}, \tag{3.9}$$
$$\phi\,(\ell_1, \ell_2) < 172^\circ, \tag{3.10}$$

where $m\!\!\!/$ is the missing mass defined by $m\!\!\!/^2 = \not{E}^2 - (\Sigma\vec{p})^2$, where the sum is over observed particles. The resulting SM background from WW production is

$$WW \to e^+e^-, \mu^+\mu^- : \ 14.4 \text{ fb},$$
$$WW \to \tau^\pm\ell^\mp \to \ell^+\ell^- : \ 19.2 \text{ fb},$$
$$WW \to \tau^+\tau^- \to \ell^+\ell^- : \ 3.7 \text{ fb},$$

where ℓ is summed over e and μ. The resulting 5σ contours are plotted as dotted lines in Fig. 3. Comparing Fig. 3(a) with Fig. 2(a) shows that LEP2 operating at $\sqrt{s} = 175$ GeV will actually have a somewhat smaller reach for the neutralino dilepton signal than LEP2 operating at $\sqrt{s} = 150$ GeV—a consequence of the WW background. In addition, for the $\tan\beta = 10$ case illustrated in Fig. 3(c), there is now *no* reach for neutralinos in the dilepton channel.

The search for $\widetilde{Z}_1\widetilde{Z}_2 \to$ jets$+\not{E}_T$ is more complicated at $\sqrt{s} = 175$ GeV than at $\sqrt{s} = 150$ GeV due not only to the WW background, but also from a background due to ZH_ℓ production. We require

$$m \text{ (detected)} < 60 \text{ GeV}, \tag{3.11}$$
$$\not{E}_T > 9 \text{ GeV}, \tag{3.12}$$
$$\not{E} > 110 \text{ GeV}, \tag{3.13}$$
$$m\!\!\!/ > 90 \text{ GeV}, \tag{3.14}$$
$$\phi\,(j_1, j_2) < 172^\circ \text{ (dijet events)}. \tag{3.15}$$

For the $\tan\beta = 2$, $\mu < 0$ case of Fig. 3(a), we find essentially no observable region. This is due to combined backgrounds from (i) $\widetilde{W}_1\widetilde{W}_1$ production, (ii) WW production, and mainly (iii) $ZH_\ell \to \nu\bar{\nu}b\bar{b}$ [see Fig. 1(b)]. As for LEP2 at $\sqrt{s} = 150$ GeV, there is again no neutralino jets$+\not{E}_T$ signal visible in Fig. 3(b). For the case of Fig.

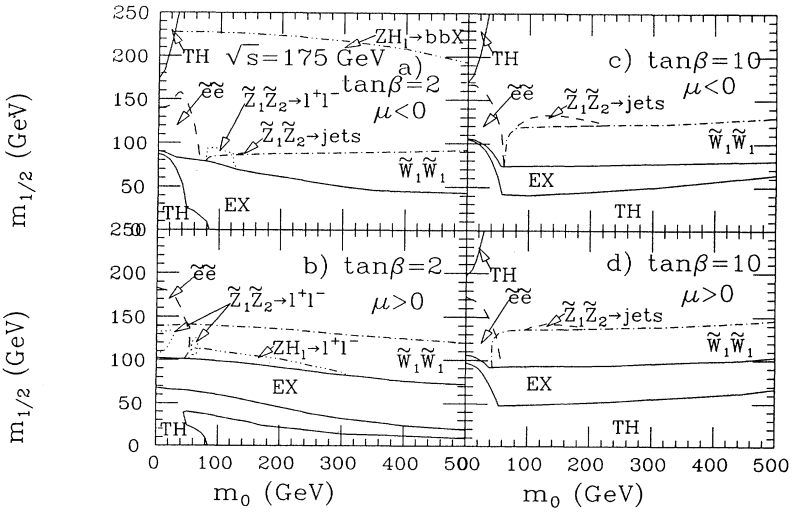

FIG. 3. Same as Fig. 2, except for $\sqrt{s} = 175$ GeV, and $\int \mathcal{L}dt = 500$ pb^{-1}.

3(c), the light Higgs scalar is too massive to be produced, and the main background comes from

$$WW \to q\bar{q}'\tau\nu_\tau \ : \ 6.0 \text{ fb}.$$

The observable region, delineated by a dashed contour, lies just beyond the reach for observation of $\widetilde{W}_1\widetilde{W}_1$. Likewise, a small region of observability is seen in Fig. 3(d).

3.4 Higgs bosons. An important consequence of the minimal SUGRA model is that the masses and couplings of the various Higgs bosons are correlated with the masses and couplings of all the rest of the supersymmetric particles, as well as with the top quark. In particular, in minimal SUGRA with large $|\mu|$ due to radiative electroweak symmetry breaking, the lightest Higgs scalar, H_ℓ, is very much like a SM Higgs boson, but with mass bounded by $m_{H_\ell} \lesssim 130$ GeV. Hence, the search for the light Higgs via $e^+e^- \to ZH_\ell$ can explore regions of the same m_0 vs $m_{1/2}$ plane that can be explored by the search for various SUSY particles.

The search for $e^+e^- \to ZH_\ell \to Zb\bar{b}$ proceeds along the same lines as the search for a SM Higgs, where $H_{\rm SM} \to b\bar{b}$. Simulations have been carried out for signal and background in a SM Higgs search (see Ref. [23]), where a discovery cross section at 3σ for $e^+e^- \to ZH_{\rm SM}$ of 200 fb was found. We convert this number to a 5σ limit for $\int \mathcal{L}dt = 500$ pb^{-1}, and take into account possible variations in the SUSY Higgs production cross section and decay branching ratio. The resulting dot-dot-dashed contour is plotted in Fig. 3(a), which probes to $m_{H_\ell} \simeq 82$ GeV. We see that by far the largest region of parameter space for this case can be scanned via the search for Higgs bosons. If, however, a Higgs signal is found, it would be difficult to distinguish in this case whether it is a SM or SUSY Higgs boson. The $\tan\beta = 2$, $\mu > 0$ case illustrated in Fig. 3(b) has in general heavier H_ℓ than the case of Fig. 3(a), and so the H_ℓ is visible in a much smaller region. In fact, in Fig. 3(b), the region of Higgs observability occurs when $ZH_\ell \to \ell^+\ell^- + \widetilde{Z}_1\widetilde{Z}_1$ occurs at the 10 event level, and the Higgs itself is dominated by invisible decay modes to $\widetilde{Z}_1$ pairs. Finally, in Figs. 3(c) and 3(d), none of the m_0 vs $m_{1/2}$ plane can be explored via Higgs searches, due to the H_ℓ being too massive.

IV. DETECTING SPARTICLES AT $E_{\rm c.m.} = 190$ AND 205 GeV

If LEP2 is operated at $\sqrt{s} = 190$ GeV, a smaller total sample of integrated luminosity ~ 300 pb^{-1} is expected to be gathered. In addition, the SM WW production cross section will increase from 17.3 pb to 19.2 pb, and the threshold for producing real ZZ events will be passed. The latter are expected to occur with a cross section of 1.1 pb.

4.1 selectrons. To evaluate selectron pair production signals at LEP2 at $\sqrt{s} = 190$ GeV, we again use the cuts (3.1)–(3.4), except for increasing the lepton energy upper limit to $E_\ell < 50$ GeV, and increasing the $\not{E}_T$ cut to $\not{E}_T > 9.5$ (10.3) for $\sqrt{s} = 190$ (205) GeV. The background from ZZ production is again computed using HELAS. The resultant SM backgrounds for dielectron+$\not{E}_T$ events are

$$WW \to e^+e^- : \ 10.4 \text{ fb},$$
$$WW \to \tau^\pm e^\mp \to e^+e^- : \ 6.1 \text{ fb},$$
$$WW \to \tau^+\tau^- \to e^+e^- : \ 0.8 \text{ fb},$$
$$ZZ \to \nu\bar{\nu}\tau^+\tau^- \to e^+e^- : \ 0.2 \text{ fb}.$$

The resultant background at $\sqrt{s} = 190$ GeV is smaller than the corresponding background for $\sqrt{s} = 175$ GeV due to sharper distributions in the forward region for the higher energy option. The 5σ region of observability is plotted in Fig. 4, and indicated again by the dashed contours. We find that selectron masses of $m_{\tilde{e}_R} \simeq 83$–$88$ GeV can be probed, depending on the mass and composition of $\widetilde{Z}_1$.

4.2 charginos. For chargino pair production at LEP2 at $\sqrt{s} = 190$ GeV, we again use the cuts (2.4)–(2.9), with the background scaled to the appropriate energy and luminosity. The regions for chargino discovery via the mixed hadronic-leptonic event structure are indicated by dot-dashed contours in Fig. 4. The corresponding

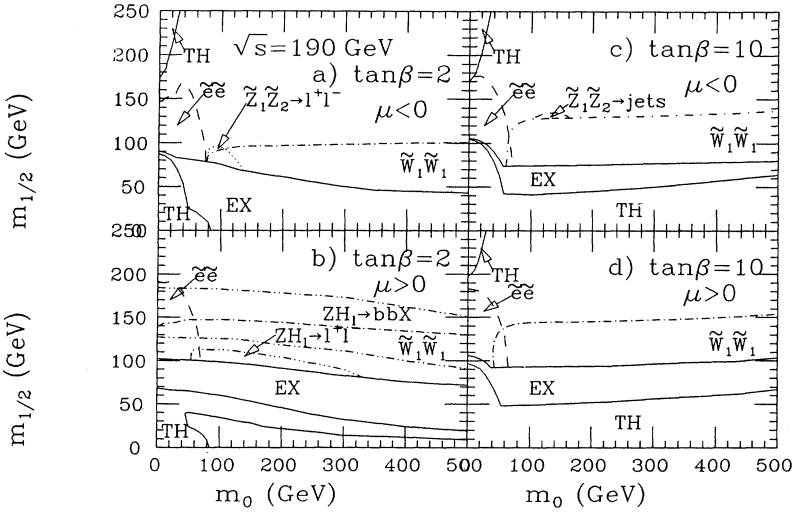

FIG. 4. Same as Fig. 2, except for $\sqrt{s} = 190$ GeV, and $\int \mathcal{L}dt = 300$ pb^{-1}.

reach in terms of $m_{\widetilde{W}_1}$ increases to $m_{\widetilde{W}_1} \sim 94$ GeV for large m_0, which is almost at the kinematic limit.

4.3 neutralinos. To search for $e^+e^- \to \widetilde{Z}_1\widetilde{Z}_2 \to \ell\bar{\ell}+\not{E}_T$ events, we require (after some optimization)

$$6 < E_\ell < 54 \text{ GeV}, \quad |\eta_\ell| < 2.5, \tag{4.1}$$

$$\not{E}_T > 9.5 \text{ GeV}, \tag{4.2}$$

$$\not{E} > 122 \text{ GeV}, \tag{4.3}$$

$$m(\ell\bar{\ell}) < 50 \text{ GeV}, \tag{4.4}$$

$$m\!\!\!/ > 106 \text{ GeV}, \tag{4.5}$$

$$\phi(\ell_1, \ell_2) < 172^\circ. \tag{4.6}$$

The SM backgrounds from WW and ZZ production are

$WW \to \ell^+\ell^-$: 20.2 fb,
$WW \to \tau^\pm\ell^\mp \to \ell^+\ell^-$: 30.6 fb,
$WW \to \tau^+\tau^- \to \ell^+\ell^-$: 6.0 fb,
$ZZ \to \nu\bar{\nu}\ell^+\ell^-$: 0 fb [due to cuts (4.4) and (4.5)],
$ZZ \to \nu\bar{\nu}\tau^+\tau^- \to \ell^+\ell^-$: 0.3 fb,

where ℓ is summed over e and μ. The 5σ contours are plotted as usual as dotted lines in Fig. 4. We see in Fig. 4(a) that the dilepton signal from $\widetilde{Z}_1\widetilde{Z}_2$ production yields only a tiny region beyond that which is explorable via chargino searches, at $\sqrt{s} = 190$ GeV. In Figs. 4(b)–4(d), only a handful of points yielding an observable dilepton signal were found. These points which fall inside the region that can be explored via chargino or selectron searches are not shown for clarity. We thus see that while the neutralino dilepton signal frequently does not expand the parameter region that might be explored at LEP2, in favorable cases, it can lead to a confirmatory signal first seen in another channel.

The search for $\widetilde{Z}_1\widetilde{Z}_2 \to$ jets$+\not{E}_T$ is complicated at $\sqrt{s} = 190$ GeV by the fact that there can be a substantial rate for $ZH_\ell \to \nu\bar{\nu}b\bar{b}$ production over much of parameter space. For the cases illustrated in Figs. 4(a) and 4(b), again, no jets $+\not{E}_T$ signal could be picked out against SM and Higgs production backgrounds. For the $\tan\beta = 10$ case of Fig. 4(c), where the H_ℓ is still too heavy to be produced, only a small slice of parameter space yielded a region where the $\widetilde{Z}_1\widetilde{Z}_2$ signal could be seen. To do so, we required

$$m(\text{detected}) < 44 \text{ GeV}, \tag{4.7}$$

$$\not{E}_T > 9.5 \text{ GeV}, \tag{4.8}$$

$$\not{E} > 126 \text{ GeV}, \tag{4.9}$$

$$m\!\!\!/ > 118 \text{ GeV}, \tag{4.10}$$

$$\phi(j_1, j_2) < 172^\circ \text{ (dijet events)}. \tag{4.11}$$

Backgrounds from all sources were then negligible, except for

$$WW \to q\bar{q}'\tau\nu_\tau \text{ : 6.1 fb.}$$

For Fig. 4(d), no regions of observability for $\widetilde{Z}_1\widetilde{Z}_2 \to$ jets$+\not{E}_T$ were found.

4.4 Higgs bosons. For LEP2 at $\sqrt{s} = 190$ GeV, we again follow the prescription outlined in Sec. III D to find regions where $ZH_\ell \to Zb\bar{b}$ is detectable, except for updating the machine energy and luminosity. For Fig. 4(a), the whole of the m_0 vs $m_{1/2}$ plane shown may be explored via the Higgs search. The discovery limit contour actually occurs around $m_{1/2} \sim 300 - 400$ GeV (shown later in Fig. 6), corresponding to Higgs boson masses of $m_{H_\ell} \simeq 93$ GeV. In Fig. 4(b), there now exists a region of $H_\ell \to b\bar{b}$ observability, indicated by the area *between* the dot-dot-dashed contours. Furthermore, $H_\ell \to \widetilde{Z}_1\widetilde{Z}_1$ is detectable below the triple-dot-dashed contours, as in Fig. 3(b). The small area between these two regions of observability is where the H_ℓ branching fraction is split up between the $b\bar{b}$ and invisible $\widetilde{Z}_1\widetilde{Z}_1$ modes. Here the Higgs signal is just slightly below our criteria for observability in either mode. However, if these criteria are relaxed slightly (to, e.g., a 4σ effect), or if the luminosity is increased, then the gap region will become observable. Finally, for the $\tan\beta = 10$ case shown in Figs. 4(c) and 4(d), the H_ℓ is again too heavy ($m_{H_\ell} \gtrsim 95$ GeV) to be seen anywhere in the plane shown.

For completeness, we show in Figs. 5(a)–5(d) the corresponding region detectable by LEP2 operating at $\sqrt{s} = 205$ GeV and integrated luminosity of 300 pb^{-1} which has been proposed as a possible upgrade option for LEP2, particularly for extending the H_ℓ reach. Since no new SM backgrounds open up, we use the same cuts as in the $\sqrt{s} = 190$ GeV case. In general, the various search regions expand somewhat from the $\sqrt{s} = 190$ GeV plot of Fig. 4. The main difference comes in the search for the light Higgs boson. In Fig. 5(a), the LEP2 reach for Higgs bosons at $\sqrt{s} = 205$ GeV has expanded to a contour at around $m_{1/2} \sim 500 - 600$ GeV. Fine-tuning arguments [24] would suggest that such a reach (which corresponds to a gluino (chargino) mass of ~ 1400 (~ 500) GeV) essentially probes all of the parameter space of weak scale supersymmetry. Such a conclusion should be viewed in perspective. First, the fine-tuning criteria are subjective. Second, as shown below, the range in $m_{1/2}$ explorable via the Higgs boson search; i.e., the correlation between m_{H_ℓ} and the gaugino mass is very sensitive to other parameters. For instance, for the $\tan\beta = 2\mu > 0$ case of Fig. 5(b), the Higgs reach has extended to around $m_{1/2} \sim 250$ GeV, although the slight gap of difficult observability persists around $m_{1/2} \sim 100 - 120$ GeV. Furthermore, LEP2 at $\sqrt{s} = 205$ GeV finally has a significant reach for the high $\tan\beta$ case of Fig. 5(c), where $e^+e^- \to ZH_\ell$ can now be seen to $m_{1/2} \sim 100$ GeV, for $m_0 < 200$ GeV. The $\tan\beta = 10$, $\mu > 0$ case of Fig. 5(d) still has no region of Higgs observability, since $m_{H_\ell} > 100$ GeV throughout the allowed plane. We thus conclude that while the increased energy of LEP2 substantially expands the parameter space region that can be explored via the Higgs boson search, nonobservation of any signal cannot unequivocally exclude even this very restricted framework even if LEP2 is operated at 205 GeV. Of course, the observation of the Higgs signal alone, while very welcome, would not serve to distinguish the SUSY framework from the SM.

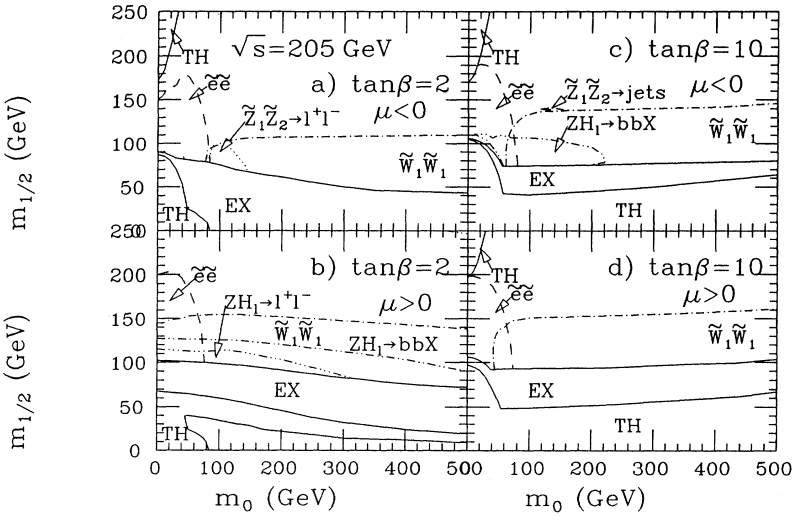

FIG. 5. Same as Fig. 2, except for $\sqrt{s} = 205$ GeV, and $\int \mathcal{L}dt = 300$ pb^{-1}.

V. OTHER MULTILEPTON SIGNALS

In addition to the more typical signals for supersymmetry at LEP2 already discussed, there exist additional signals which have rarely been addressed in the literature. These include signals containing three or four isolated leptons. For example, 3ℓ+ jets+$\not{E}$ can come from $\tilde{\nu}_\ell\bar{\tilde{\nu}}_\ell$ production, where $\tilde{\nu}_\ell \to \nu_\ell\tilde{Z}_2 \to \nu_\ell e\bar{e}\tilde{Z}_1$, whereas $\bar{\tilde{\nu}}_\ell \to e\widetilde{W}_1 \to eq\bar{q}'\tilde{Z}_1$. Likewise, $4\ell + \not{E}$ events can come from $\tilde{e}_i\bar{\tilde{e}}_j$ ($i,j = L$ or R) production, where, for instance, $\tilde{e}_i \to \tilde{Z}_2 e$ followed by $\tilde{Z}_2 \to e\tilde{e}_R \to e\bar{e}\tilde{Z}_1$, while the original $\tilde{e}_j \to e\tilde{Z}_1$, $\tilde{Z}_2\tilde{Z}_2 \to \ell\bar{\ell}\tilde{Z}_1 + \ell'\bar{\ell}'\tilde{Z}_1$, and $\tilde{\nu}_\ell\bar{\tilde{\nu}}_\ell$ production, where sneutrinos decay via $\tilde{\nu}_\ell \to \nu_\ell\tilde{Z}_2 \to \nu_\ell e\bar{e}\tilde{Z}_1$ or $\tilde{\nu}_\ell \to \ell\widetilde{W}_1 \to \ell\ell'\nu_{\ell'}\tilde{Z}_1$. The above reactions generally occur within subsets of the regions of parameter space already delineated in Secs. II–IV, and so give no additional reach for supersymmetry. The detection of such events is nonetheless important since it could serve to test the details of the underlying model.

As an example, in Fig. 6 we delineate regions of parameter space where $4\ell + \not{E}$ events are observable, assuming the $\sqrt{s} = 190$ GeV option for LEP2. We require

$$E_\ell > 3 \text{ GeV}, \quad |\eta_\ell| < 2.5, \tag{5.1}$$

$$\not{E}_T > 9.5 \text{ GeV}, \tag{5.2}$$

and then require at least 5 signal events for observability, since SM backgrounds should be tiny because ZZ production and direct decays to e or μ pairs can be easily vetoed, and ZZ or $ZH_\ell \to 4\tau \to 4\ell$ cross section is small. The resulting regions are plotted in Figs. 6(a)–6(d). In Fig. 6(a), there is unfortunately only a tiny region of 4ℓ observability, while in Fig. 6(b) there is a substantial region, outlined by the dashed contour. Within the dashed contour, the dotted contours delineate which reaction dominantly contributes to the signal. In Fig. 6(b), $\tilde{e}_L\tilde{e}_R$ and $\tilde{Z}_2\tilde{Z}_2$ are the dominant production mechanisms over most of the observable region, with $\tilde{\nu}_\ell\bar{\tilde{\nu}}_\ell$ contributing dominantly in a smaller region. For the $\tan\beta = 10$ cases of Figs. 6(c) and 6(d), $\tilde{\nu}_\ell\bar{\tilde{\nu}}_\ell \to 4\ell$ dominates for $60 < m_0 < 100$ GeV. For reasons of brevity, we do not

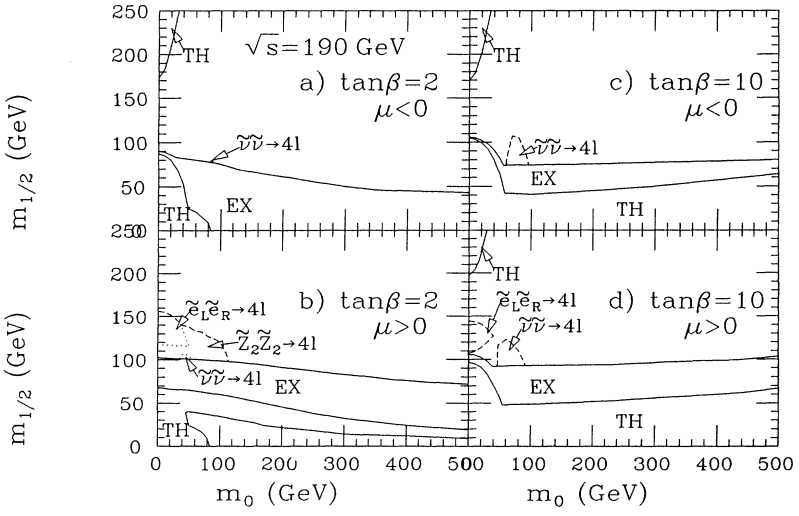

FIG. 6. A plot similar to Fig. 4 (for $\sqrt{s} = 190$ GeV, and $\int \mathcal{L}dt = 300$ pb^{-1}), except we show regions yielding at least five events containing four isolated leptons that do not come from Z pairs. The complete region where there are 4ℓ signals from all sources is outlined by the dashed contours; the dotted contours delineate regions where most or all of the signal comes from the particular reaction shown on the figure.

show regions where trilepton signals occur at observable rates, nor do we show the energy dependence of the 3ℓ and 4ℓ signals.

VI. COMPARISON OF VARIOUS LEP2 ENERGY UPGRADE OPTIONS AND COMPARISON WITH TEVATRON MI

We show in Fig. 7 the cumulative search contours for LEP2 energies of $\sqrt{s} = 175$, 190, and 205 GeV, with respective integrated luminosities of $\int \mathcal{L}dt = 500$, 300, and 300 pb^{-1}. The contours are composites of those shown in Figs. 3–5, with some tiny additional regions added in where, for instance, overlapping slepton and neutralino signals can increase the SUSY discovery reach. It is clear to see that the energy increase from $\sqrt{s} = 175$ GeV, to 190 and 205 GeV results in increased detectability for charginos from roughly 87 GeV, to 95 GeV and 102 GeV, respectively (for m_0 large). Likewise, in the small m_0 region ($m_0 \simeq \frac{m_{1/2}}{\sqrt{3}}$), selectron masses of $m_{\tilde{\ell}_R} \simeq 82$, 88 and 96 GeV can be probed. This is a clear argument for LEP2 to try to attain the highest energy option. An exception to this does occur, however, for observation of the $\widetilde{Z}_1\widetilde{Z}_2$ reaction. As can be seen in the $m_0 \sim 100$ GeV region of Fig. 7(a), all three (and even the $\sqrt{s} = 150$ GeV option) energy upgrades have roughly equivalent reach. This is due to the fact that LEP2 operating at a reduced energy can have a similar or perhaps even better chance for observing neutralino pairs than the higher energy options. This situation occurs because $\widetilde{Z}_1\widetilde{Z}_2$ production has a very small cross section, and the additional backgrounds from WW, ZZ, and ZH_ℓ production at higher energies can swamp the tiny neutralino pair signal. In addition, supersymmetric processes such as $\widetilde{W}_1\widetilde{W}_1$ production can mask some of the region where $\widetilde{Z}_1\widetilde{Z}_2$ might have otherwise been visible.

In Fig. 7, in addition to the cumulative contours for the three LEP2 energy and luminosity options, we have as well plotted the approximate reach of experiments operating at the Fermilab $p\bar{p}$ collider in the Main Injector (MI) era. The Tevatron MI is expected to turn on around 1999, at $\sqrt{s} = 2$ TeV, and it is expected to accumulate ~ 1 fb^{-1} of integrated luminosity per year. Recently, the reach in $m_{\tilde{g}}$ has been calculated for searches in the multijet+$\not{E}_T$ channel which results from $p\bar{p} \to \tilde{g}\tilde{g}$, $\tilde{g}\tilde{q}$ and $\tilde{q}\tilde{q}$ production [11,25]. It was found that the Tevatron MI could probe to $m_{\tilde{g}} \sim 200-270$ GeV ($m_{\tilde{q}} \gg m_{\tilde{g}}$), or $m_{\tilde{g}} \sim 265 - 350$ GeV ($m_{\tilde{q}} \sim m_{\tilde{g}}$). We combine the more optimistic of these values [11] with the recent calculation of the Tevatron MI reach for SUSY via trileptons and dileptons from chargino-neutralino production [13] (see also [11,14]). The resultant small dashed contours are shown in Fig. 7, and labeled by MI. For all four cases shown, it is clear that LEP2 will have a larger reach for minimal SUGRA in the large m_0 region, due to searches for chargino pairs. In addition, LEP2 can probe regions of small m_0 not accessible to the MI, via the search for selectrons. However, in the intermediate region of $m_0 \sim 100-200$ GeV, Tevatron MI experiments can have a superior reach to LEP2, mainly via the search for $\widetilde{W}_1\widetilde{Z}_2 \to 3\ell + \not{E}_T$ events. These contours clearly illustrate the complementary capabilities of LEP2 e^+e^- and Tevatron MI $p\bar{p}$ colliders.

In Figs. 8(a) and 8(b), we show the regions of m_0 vs $m_{1/2}$ space explorable via Higgs searches, for the two $\tan\beta = 2$ cases. For $\tan\beta = 10$, $\mu < 0$ case, the light Higgs is too heavy to be observed at any of the LEP2 energy-luminosity options except for $\sqrt{s} = 205$ GeV, which is plotted in Fig. 5(c). For the $\tan\beta = 10$, $\mu > 0$ case, the light Higgs is too heavy to be observed at *any* of the considered LEP2 energy or luminosity options. For the $\sqrt{s} = 150$ GeV option, of course, no Higgs signal is visible beyond LEP1 bounds. In Fig. 8(a), the $\sqrt{s} = 175$ GeV energy option can explore up to $m_{H_\ell} \sim 82$ GeV, which covers a significant portion of the $\tan\beta = 2$, $\mu < 0$, $A_0 = 0$ parameter space — well beyond the regions for any SUSY particle searches. The modest energy increase to $\sqrt{s} = 190$ GeV considerably increases the reach in the SUGRA space explorable via the Higgs search. This is primarily because H_ℓ cannot become too

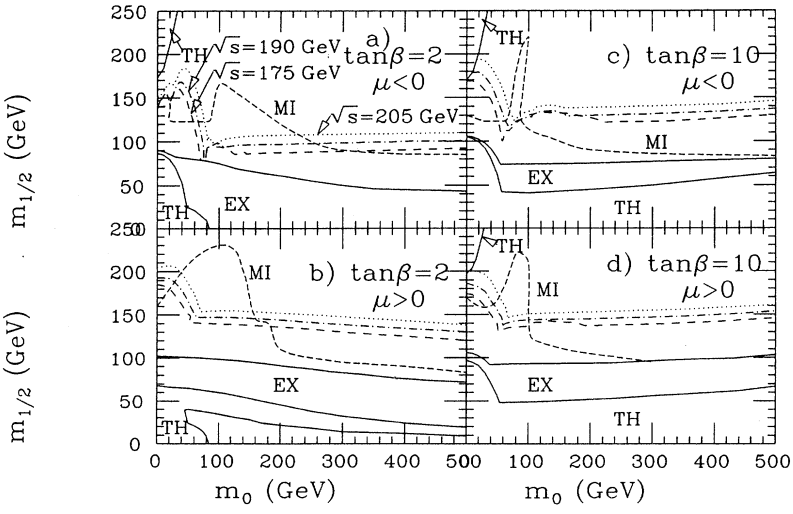

FIG. 7. Cumulative reach of various LEP2 upgrade options for supersymmetric particles (excluding Higgs bosons), for $\sqrt{s} = 175$ GeV and $\int \mathcal{L}dt = 500$ pb^{-1} (dashed), $\sqrt{s} = 190$ GeV and $\int \mathcal{L}dt = 300$ pb^{-1} (dot-dashed), and $\sqrt{s} = 205$ GeV and $\int \mathcal{L}dt = 300$ pb^{-1} (dotted). Also shown for comparison is the combined reach of Tevatron Main Injector era experiments ($\sqrt{s} = 2$ TeV and $\int \mathcal{L}dt = 1000$ pb^{-1}) (dashed curve labeled by MI).

heavy within this (and many other) model framework(s). The $\sqrt{s} = 205$ GeV option can probe essentially the whole range of parameters allowed by fine-tuning arguments [24] for negative values of μ. If $\mu > 0$, the region probed via the Higgs search is significantly smaller. We see from Fig. 8(b) that the $\sqrt{s} = 175$ GeV LEP2 option could only explore a small region of SUGRA space, and that via the invisible Higgs signal. The energy increase to $\sqrt{s} = 190$ GeV would not increase the invisible Higgs region significantly, but would probe the interior of the dot-dashed region via a $ZH_\ell \to Zb\bar{b}$ search. An increase of energy to $\sqrt{s} = 205$ GeV would substantially increase the region seeable via $ZH_\ell \to Zb\bar{b}$, but would leave the lower gap region around $m_{1/2} \sim 100$ GeV still on the edge of observability in both visible and invisible Higgs boson decay channels.

We conclude that nonobservation of a Higgs signal would rule out a huge region of this particular plane particularly if $\mu < 0$. It should, however, be kept in mind that the detection of the Higgs boson signal would not be conclusive evidence for SUSY, since H_ℓ is essentially indistinguishable from the SM Higgs boson. Higgs boson detection via its invisible mode, which is possible for positive values of μ, would of course imply the existence of a non-SM Higgs sector.

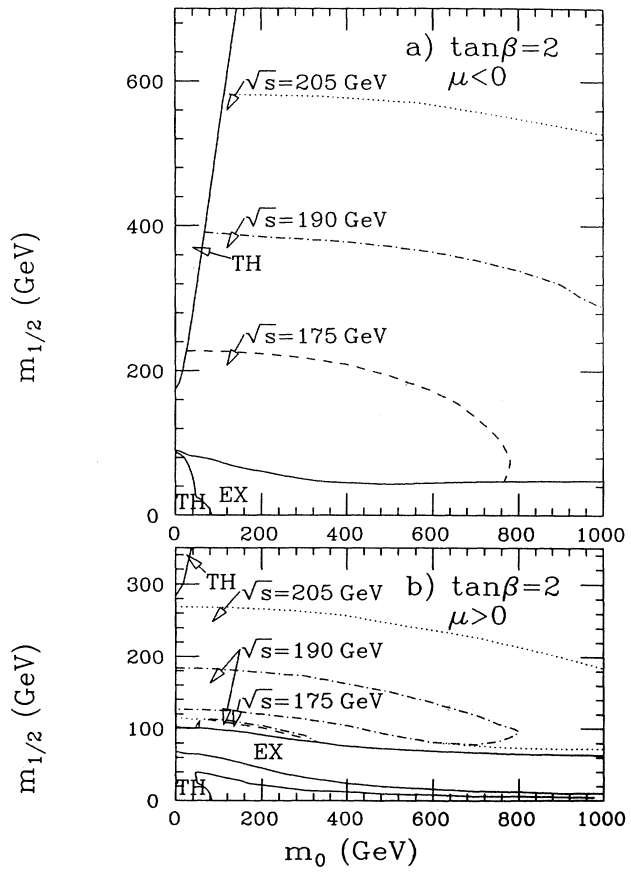

FIG. 8. Reach of various LEP2 upgrade options for the lightest Higgs boson H_ℓ, for the $\sqrt{s} = 175$ GeV (dashes), $\sqrt{s} = 190$ GeV (dot-dashed), and $\sqrt{s} = 205$ GeV cases (dots), with an integrated luminosity as in Fig. 7 for $\tan\beta = 2$ and (a) $\mu < 0$ and (b) $\mu > 0$.

VII. NEUTRALINO SEARCH IN THE SUGRA-INSPIRED MSSM ($|\mu|$ FREE CASE)

All of the preceding analysis has been performed within the framework of the minimal SUGRA model which, because of the assumed symmetries of dynamics at the grand unified theory (GUT) scale, is determined by just a few parameters renormalized at around the same scale. The diversity of sparticle masses and couplings, renormalized at the weak scale relevant for phenomenology, then arises via renormalization effects when common GUT scale mass and coupling parameters are evolved down to the weak scale. As discussed in Sec. I, these same radiative corrections can lead to the observed pattern of electroweak symmetry breaking, provided GUT scale parameters are chosen within certain ranges: then, the superpotential Higgs mass μ is determined up to a sign, since μ^2 is tuned to give the correct value of M_Z.

Despite the fact that SUGRA models provide an attractive and economic framework, it should be kept in mind that any of the underlying assumptions could prove to be incorrect. Indeed many theoretical and experimental analyses have been cast within the framework of the SUGRA-inspired MSSM framework, where it is generally assumed that the soft-breaking gaugino masses M_1, M_2, and M_3 are related as in a GUT model, and that the squark and slepton masses originate from a universal GUT scale soft-breaking term m_0 [26]. These requirements are easily implemented via simple formulae relating squark, slepton, and gluino masses. The additional relationships between the Higgs boson masses, the A parameters, and the electroweak symmetry breaking requirement [which usually requires a complete, coupled renormalization group equation (RGE) solution] are then neglected, so that m_{H_p}, A_t, and μ are left as free parameters. The resulting model maintains some of the important mass relationships contained in minimal SUGRA, but then has additional parameters, giving it more generality, but also making parameter space scans more tedious.

What are the main effects of relaxing these conditions for LEP phenomenology? In minimal SUGRA, generally $|\mu| \gg M_1$, M_2, and M_W, which results in gauginolike $\widetilde{W}_1, \widetilde{Z}_1$, and $\widetilde{Z}_2$. Then, the couplings of the two lighter neutralinos (which are likely to be kinematically accessible at colliders) to the Z boson is strongly suppressed, so that their production by e^+e^- collisions is also strongly suppressed, particularly when selectrons are heavy (see Fig. 1). This is not true for lighter charginos which in fact have enhanced SU(2) triplet couplings to the Z, and which, of course, also couple to photons. If we allow that we do not know the high scale dynamics, and so, relax the constraints from radiative electroweak symmetry breaking, μ^2 can be rather small, so that the lighter charginos and neutralinos can be Higgsino-like. In this case, the neutralino cross section at LEP2 may be larger by orders of magnitude (recall Higgsinos have gauge couplings to

Z) relative to the SUGRA case, while that of charginos and other charged sparticles or sneutrinos is comparatively unaffected. As a result, neutralino phenomenology may be very different, while the phenomenology of charginos and sleptons is roughly as discussed above [27].

Indeed earlier studies within the SUGRA-inspired MSSM framework have shown that the search for chargino pairs (and also sleptons) would generally proceed as discussed earlier for the minimal SUGRA model, and in general, charginos ought to be visible if their production is kinematically allowed [7,8,28]. The case for neutralino pair production, however, can be quite different. When $|\mu|$ is small, as allowed in the SUGRA-inspired MSSM, then $\widetilde{Z}_1\widetilde{Z}_2$ production can take place via the s-channel Z exchange graph, and the total $\widetilde{Z}_1\widetilde{Z}_2$ production cross section can be comparable to the total $\widetilde{W}_1\widetilde{W}_1$ cross section, even if selectrons are quite heavy. These neutralino total cross sections have recently been displayed in the μ vs M_2 plane [29,30], although without explicit simulation and background evaluation. Because neutralino production rates are extremely sensitive to the assumption of the radiative symmetry breaking mechanism, and because relatively little work has been done on the prospects of detecting these signals at e^+e^- colliders, we felt it worthwhile to single out neutralino signals for a closer investigation. In the interest of brevity, and because this analysis is outside the main theme of this paper, we illustrate this for just one center-of-mass energy $\sqrt{s} = 190$ GeV.

To this end, we plot in Fig. 9 the cross section after cuts (see Sec. IV) from all SUSY and Higgs boson sources of $\ell\bar{\ell} + \not{E}_T$, ℓ + jets + $\not{E}_T$ and, finally, jets + $\not{E}_T$ events for the $\sqrt{s} = 190$ GeV option of LEP2. Chargino and neutralino production and subsequent decays are the primary source of these events in the figure, where for definiteness, we have chosen $m_{\tilde{g}} = 600$ GeV, $m_{\tilde{q}} = 1000$ GeV (this roughly corresponds to $m_0 \sim 850$ GeV, $m_{1/2} \sim 220$ GeV in the SUGRA case—a look at Fig. 4 shows that there would be no observable SUSY signal within this

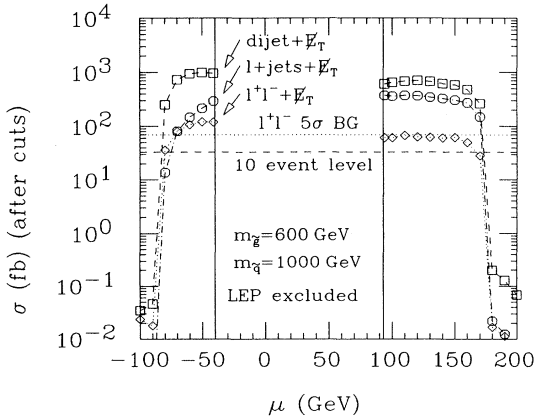

FIG. 9. Cross section for various event topologies for LEP2 at $\sqrt{s} = 190$ GeV, after the cuts of Sec. IV, for supersymmetric signals vs the μ parameter. Here, μ is taken as a free parameter because the requirement of radiative electroweak symmetry breaking has been dropped.

framework for parameters in this range), and $\tan\beta = 2$. The sleptons, whose masses are fixed by SUGRA relations, have masses ~ 850 GeV, and so are too heavy to be of direct interest. The weak scale A parameters and m_{H_p} are chosen to be -1000 GeV and 500 GeV, respectively, but our results are insensitive to this choice. The band between the vertical lines is excluded by the nonobservation of any SUSY signal or deviations in the Z line shape in experiments at LEP. We see that these signals are at or above the 5σ level for a substantial region of small μ^2. Several comments are worthy of note.

When $|\mu|$ is large, as is typical in SUGRA models, $\widetilde{W}_1\widetilde{W}_1$ and $\widetilde{Z}_1\widetilde{Z}_2$ production is kinematically not allowed, but as $|\mu|$ decreases, $m_{\widetilde{W}_1}$ and $m_{\widetilde{Z}_{1,2}}$ also decrease until their production becomes kinematically accessible. Single lepton production can only come from chargino decays (except when a lepton from the decay of a neutralino escapes undetected) while chargino and neutralino production can both contribute to the dilepton and dijet signals.

For values of μ in the central region, where the cross sections are substantial, we see from the relative size of the 1ℓ and the other cross sections that chargino and neutralino production indeed contribute comparable amounts as anticipated.

For positive values of μ, the chargino is typically lighter than when μ is negative, and has the same magnitude. This is reflected in the relatively larger single lepton cross sections in this case compared to $\mu < 0$.

The relative contributions of the various SUSY processes to the dilepton and dijet signals is sensitive to the parameters. For the choice in the figure, particularly at the large $|\mu|$ edge where the signals drop rapidly, the bulk of the neutralino contribution comes from $\widetilde{Z}_1\widetilde{Z}_3$ production: This is because the $\widetilde{Z}_3$ tends to have a substantially larger Higgsino component than $\widetilde{Z}_2$ for the particular parameter choice. The cross sections drop rapidly once $\widetilde{Z}_1\widetilde{Z}_3$ production becomes kinematically forbidden. At this point $\widetilde{Z}_1\widetilde{Z}_2$ production is still allowed which is why the cross sections do not go to zero; the smallness of this cross section reflects the large suppression of the $Z\widetilde{Z}_1\widetilde{Z}_2$ coupling. The crossover between the single lepton and the dilepton curves for large negative values of μ occurs because $\widetilde{W}_1\widetilde{W}_1$ production becomes kinematically inaccessible even when $\widetilde{Z}_1\widetilde{Z}_3$ production continues to remain allowed.

We have just seen that if lighter neutralinos are Higgsino-like, they will lead to characteristic signals at rates comparable to chargino production. Since these signals can also come from chargino production, it is reasonable to ask if one can distinguish chargino production alone from chargino and neutralino production. Several possibilities come to mind. (i) Neutralino production does not lead to single lepton topologies except when a lepton escapes experimental detection: observation of a substantial rate for this would point to charginos as the source of such events. (ii) Chargino pair production is as likely to yield like-flavor as unlike-flavor dilepton pairs. An excess of e^+e^- and $\mu^+\mu^-$ relative to $e^\pm\mu^\mp$

events would likely indicate the simultaneous production of charginos along with sleptons or neutralinos. Slepton production generally occurs at a significantly larger rate and (unless sleptons can also decay to charginos) does not result in jet(s) plus $\not{E}_T$ events. (iii) The mass of $\ell^+\ell^-$ pairs from $\widetilde{Z}_i\widetilde{Z}_1$ production is bounded above by $m_{\widetilde{Z}_i} - m_{\widetilde{Z}_1}$ while the corresponding distribution from chargino pair production is expected to be much broader. Unfortunately, this does not always prove to be useful. We have checked, for example, that for positive values of μ where the chargino is significantly lighter than $\widetilde{Z}_2$ the distributions look crudely similar, and so may be difficult to distinguish. For $\mu < 0$ this distinction might well be possible.

To sum up the results of this section, neutralino production rates are small in supergravity models with radiative symmetry breaking unless sleptons are also light. If, however, we relax the radiative symmetry breaking ansatz, neutralino production may be increased by orders of magnitude, and an observable signal might be possible. In this case, it would be interesting to see if neutralino events can be distinguished from chargino events which would occur at similar rates.

VIII. SUMMARY

We have used ISAJET to examine signals for various supersymmetric processes that might be accessible at LEP2. Our study differs from most earlier LEP2 studies in that we work within the economic minimal SUGRA framework which is fixed in terms of just four parameters along with the sign of the superpotential Higgsino mass parameter (μ). This introduces correlations between various sparticle masses which, in turn, lead to new features (that are absent in the supergravity-inspired MSSM framework) in the behavior of different cross sections as a function of model parameters. Also, several SUSY reactions may be kinematically accessible at the same time. We have devised cuts to separate SUSY and Higgs boson signals from SM backgrounds, and also to differentiate as much as possible between various signal processes.

Our purpose has been to assess the reach of LEP2 and compare four different options for an energy upgrade. The details of our computations are given in Secs. II–IV, and in Figs. 2–5 where the regions of the m_0-$m_{1/2}$ plane that might be probed via different channels are shown. Generally speaking, increasing the center-of-mass energy increases the reach in $m_{1/2}$ by about (50–70)% of the increase in energy as illustrated in Fig. 7, where the composite region of the plane that can be probed via any SUSY channel is shown. There is, however, an important exception: if LEP2 is run below the WW threshold, SM backgrounds are greatly reduced so that the $\widetilde{Z}_1\widetilde{Z}_2$ reaction might be more easily seen than at LEP2 operating at higher energies. Figure 7 also shows for comparison the reach of the Main Injector upgrade of the Tevatron. We see that there are regions of parameter space where the Tevatron upgrade significantly outperforms even the highest energy option considered for LEP2, while in other regions, exactly the opposite is true. This illustrates the complementarity between e^+e^- and hadron colliders.

Unlike the case of sparticle searches, where increasing LEP2 energy leads to modest increase in the SUSY reach of the machine, a relatively small increase in the machine energy results in a significantly larger reach when probing the Higgs sector. This stems from the well-known fact that the mass of the lightest neutral Higgs scalar is bounded by $\sim$ 130 GeV within this framework, and is illustrated in Fig. 8. A definitive nonobservation of *any* Higgs boson signal (including the missing energy signal from $H_\ell \to \widetilde{Z}_1\widetilde{Z}_1$ decays) would result in stringent restrictions on the model parameters. Unfortunately, however, while the observation of a Higgs boson signal in one of the SM modes would be most welcome, it would not (unless we are extremely lucky) serve to distinguish the SUSY framework from the SM. From this point of view, there appears to be no substitute for a direct observation of sparticles. Motivated by the fact that neutralino production rates can be very different from their SUGRA model values if they contain substantial Higgsino components, and that the mechanism for electroweak symmetry breaking is essentially unknown, in Sec. VII we relax the radiative symmetry breaking constraint which fixes $|\mu|$ to be large, and forces the lighter neutralinos to be gauginolike. Our main results are illustrated in Fig. 9, where it is shown that neutralino cross sections could become comparable to those of charginos, although there are only small regions of parameter space where neutralino signals might be observable and where chargino pair production is kinematically forbidden.

In summary, we have examined the prospects for the detection of supersymmetry at various energy upgrade options of LEP2 within the framework of the minimal supergravity model. Because of the underlying correlations between sparticle masses, different reactions probe different regions of the parameter space. The Fermilab Main Injector upgrade that is expected to become operational just before the turn of the century is complementary to LEP2 upgrades in that both facilities can probe significant ranges of parameters where there are no observable signals at the other facility.

ACKNOWLEDGMENTS

We thank M. Corden and C. Georgiopoulos for discussions, and G. Giudice and M. Mangano of the LEP2 SUSY working group for discussions and motivation. H.B. thanks U. Nauenberg and the University of Colorado at Boulder for hospitality and motivation while upgrading ISAJET. This research was supported in part by the U.S. Department of Energy under Grant Nos. DE-FG-05-87ER40319 and DE-FG-03-94ER40833.

[1] See, e.g., G. Barbiellini *et al.*, in *Physics at LEP*, LEP Jamboree, Geneva, Switzerland, 1985, edited by J. Ellis and R. Peccei (CERN Report No. 86-02, Geneva, Switzerland, 1986); see also *Proceedings of the ECFA Workshop on LEP 200*, Aachen, Germany, 1986, edited by A. Böhm and W. Hoogland (CERN Report No. 87-08, Geneva, Switzerland, 1987).

[2] For phenomenological reviews of SUSY, see H. P. Nilles, Phys. Rep. **110**, 1 (1984); H. Haber, and G. Kane, *ibid.* **117**, 75 (1985); X. Tata, in *The Standard Model and Beyond*, edited by J. E. Kim (World Scientific, Singapore, 1991), p. 304; V. Barger and R. J. N Phillips, in *Recent Advances in the Superworld*, Proceedings of the Workshop, Woodlands, Texas, 1993, edited by J. Lopez and D. Nanopoulos (World Scientific, Singapore, 1994); R. Arnowitt and P. Nath, *Proceedings of the VII J. A. Swieca Summer School*, Brazil, (World Scientific, Singapore, 1994); see also *Properties of SUSY Particles* Proceedings of the 23rd INFN Eloisatron Project Workshop, Erice, Italy, 1992, edited by L. Cifarelli and V. Khoze (World Scientific, Singapore, 1993).

[3] For a recent phenomenological review, see H. Baer *et. al.*, in *Electroweak Symmetry Breaking and Beyond the Standard Model*, edited by T. Barklow, S. Dawson, H. Haber, and J. Siegrist (World Scientific, Singapore, to be published).

[4] ALEPH Collaboration, D. Decamp *et al.*, Phys. Rep. **216**, 253 (1992); DELPHI Collaboration, P. Abreu *et al.*, Phys. Lett. B **247**, 157 (1990); L3 Collaboration, O. Adriani *et al.*, Phys. Rep. **236**, 1 (1993); OPAL Collaboration, M. Akrawy *et al.*, Phys. Lett. B **240**, 261 (1990); for a review, see G. Giacomelli and P. Giacomelli, Riv. Nuovo Cimento **16**, 1 (1993).

[5] Particle Data Group, L. Montanet *et al.*, Phys. Rev. D **50**, 1173 (1994).

[6] D0 Collaboration, S. Abachi *et al.*, Phys. Rev. Lett. **75**, 618 (1995); CDF Collaboration, F. Abe *et al.*, *ibid.* **69**, 3439 (1992).

[7] C. Dionisi *et al.*, in *Proceedings of ECFA Workshop on LEP 200* [1]; C. Dionisi and M. Dittmar, in *Proceedings of the Workshop on Physics at Future Accelerators*, La Thuile, Italy, 1987, edited by J. H. Mulvey (CERN Report No. 87-07, Geneva, Switzerland, 1987); J-F. Grivaz, in *Properties of SUSY Particles* [2].

[8] M. Chen, C. Dionisi, M. Martinez, and X. Tata, Phys. Rep. **159**, 201 (1988).

[9] J. Lopez, D. Nanopoulos, H. Pois, X. Wang, and A. Zichichi, Phys. Rev. D **48**, 4062 (1993).

[10] H. Baer, C. Kao, and X. Tata, Phys. Rev. D **48**, 2978 (1993); T. Tsukamoto, K. Fujii, H. Murayama, M. Yamaguchi, and Y. Okada, *ibid.* **51**, 3153 (1995); J. Lopez, D. Nanopoulos, G. Park, X. Wang, and A. Zichichi, *ibid.* **50**, 2164 (1994); H. Baer, M. Drees, C. Kao, M. Nojiri, and X. Tata, *ibid.* **50**, 2148 (1994).

[11] T. Kamon, J. Lopez, P. McIntyre, and J. T. White, Phys. Rev. D **50**, 5676 (1994).

[12] H. Baer, C. H. Chen, R. Munroe, F. Paige, and X. Tata, Phys. Rev. D **51**, 1046 (1995).

[13] H. Baer, C. H. Chen, C. Kao, and X. Tata, Phys. Rev. **D 52**, 1565 (1995).

[14] S. Mrenna, G. Kane, G. Kribs, and J. Wells, University of Michigan Report No. UM-TH-95-14, 1995 (unpublished).

[15] K. Inoue, A. Kakuto, H. Komatsu, and H. Takeshita, Prog. Theor. Phys. **68**, 927 (1982); **71**, 413 (1984).

[16] L. Ibañez and G. Ross, Phys. Lett. **110B**, 215 (1982); L. Ibañez, *ibid.* **118B**, 73 (1982); J. Ellis, D. Nanopoulos, and K. Tamvakis, *ibid.* **121B**, 123 (1983); L. Alvarez-Gaumé, J. Polchinski, and M. Wise, Nucl. Phys. **B121**, 495 (1983); G. Gamberini, G. Ridolfi, and F. Zwirner, *ibid.* **B331**, 331 (1990).

[17] See, e.g., R. Arnowitt and P. Nath, Ref. [2].

[18] F. Paige and S. Protopopescu, in *Supercollider Physics*, edited by D. Soper (World Scientific, Singapore, 1986), p. 41; H. Baer, F. Paige, S. Protopopescu, and X. Tata, in *Proceedings of the Workshop on Physics at Current Accelerators and Supercolliders*, edited by J. Hewett, A. White, and D. Zeppenfeld (Argonne National Laboratory, Argonne, 1993).

[19] H. Baer, J. Sender, and X. Tata, Phys. Rev. D **50**, 4517 (1994).

[20] For a gauginolike chargino, the ALEPH experiment has obtained a lower bound of 47 GeV, slightly better than the general bound cited in Sec. I.

[21] See J-F. Grivaz, in *Properties of SUSY Particles* [2].

[22] HELAS: Helicity amplitude subroutines for Feynman Diagram Evaluations, H. Murayama, I. Watanabe, and K. Hagiwara, KEK Report No. KEK-91-11, 1992 (unpublished).

[23] See, e.g., A. Sopczak, Int. J. Mod. Phys. A **9**, 1747 (1994).

[24] R. Barbieri and G. Giudice, Nucl. Phys. **B306**, 63 (1988); G. Anderson and D. Castaño, Phys. Rev. D **52**, 1693 (1995), present an updated measure of fine-tuning, and associated bounds on sparticle masses.

[25] H. Baer, C. Kao, and X. Tata, Ref. [10], and Phys. Rev. D **51**, 2180 (1995).

[26] In principle, each of the soft gaugino masses as well as the soft SUSY-breaking masses of each SU(3) $\times$SU(2)$\times$ U(1) multiplet should be taken as an independent parameter. The resulting proliferation of parameters would make phenomenological analyses impossible. The SUGRA GUT-inspired assumptions for these masses make these analyses tractable and serve to test the sensitivity of the resulting signals to at least some of the GUT scale assumptions.

[27] Cross sections of sparticles with nontrivial electroweak quantum numbers are changed by factors of order unity by changes of mixing angle. Also, there can be kinematic effects because of differences in sparticle masses. An important effect for chargino phenomenology in the Higgsino region is that for $M_1, M_2 \gg \mu, M_W$, $m_{\widetilde{W}_1} \simeq m_{\widetilde{Z}_1} \simeq m_{\widetilde{Z}_2}$, so that the decay products of charginos and neutralinos tend to be rather soft.

[28] J. Feng and M. Strassler, Phys. Rev. D **51**, 4661 (1995).

[29] A. Bartl, H. Fraas, W. Majerotto, and B. Mosslacher, Z. Phys. C **55**, 257 (1992); see also talk by W. Majerotto, in *Properties of SUSY Particles* [2].

[30] S. Ambrosanio and B. Mele, Rome Report No. ROME1-1094/95, 1995 (unpublished).